Case Studies in Thermal Engineering 61 (2024) 104993

Contents lists available at ScienceDirect

Case Studies in Thermal Engineering

journal homepage: www.elsevier.com/locate/csite

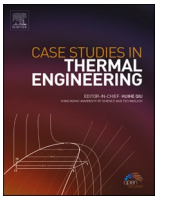

Experimental investigation on the effects of zinc oxide and goethite as additives in a diesel engine fueled by pure palm oil

Rico Aditia Prahmana [a,b,c], Prihadi Setyo Darmanto [b,l], Firman Bagja Juangsa [b,l,*], Iman Kartolaksono Reksowardojo [b,g,**], Tirto Prakoso [d,l], Jooned Hendrarsakti [b,l], Zido Yuwazama [e], Azaria Haykal Ahmad [m], Teuku Meurah Indra Riayatsyah [c], Achmad Gus Fahmi [f], Arridina Susan Silitonga [h,i], Samsu Dlukha Nurcholik [j,k]

[a] *Doctoral Program of Mechanical Engineering, Faculty of Mechanical and Aerospace Engineering, Institut Teknologi Bandung, 40132, Bandung, Indonesia*
[b] *Thermal Science and Engineering Research Group, Faculty of Mechanical and Aerospace Engineering, Institut Teknologi Bandung, 40132, Bandung, Indonesia*
[c] *Study Program of Mechanical Engineering, Faculty of Industrial Technology, Institut Teknologi Sumatera, 35365, South Lampung, Indonesia*
[d] *Department of Chemical Engineering, Faculty of Industrial Technology, Institut Teknologi Bandung, 40132, Bandung, Indonesia*
[e] *Master Program of Mechanical Engineering, Faculty of Mechanical and Aerospace Engineering, Institut Teknologi Bandung, 40132, Bandung, Indonesia*
[f] *Study Program of Cosmetic Engineering, Faculty of Industrial Technology, Institut Teknologi Sumatera, 35365, South Lampung, Indonesia*
[g] *Study Program of Mechanical Engineering, Faculty of Industrial Technology, Universitas Pertamina, 12220, Jakarta, Indonesia*
[h] *Centre for Technology in Water and Wastewater, School of Civil and Environmental Engineering, Faculty of Engineering and Information Technology, University of Technology Sydney, NSW, 2007, Australia*
[i] *Center of Renewable Energy, Department of Mechanical Engineering, Politeknik Negeri Medan, 20155, Medan, Indonesia*
[j] *Department of Naval Architecture, Institut Teknologi Kalimantan, 76127, Balikpapan, Indonesia*
[k] *Research Center of Marine Systems Emission Control, Institut Teknologi Kalimantan, 76127, Balikpapan, Indonesia*
[l] *Research Centre for New and Renewable Energy, Institut Teknologi Bandung, 40132, Bandung, Indonesia*
[m] *Department of Mechanical Engineering, The University of Tokyo, 7-3-1 Hongo, Bunkyo-ku, Tokyo 113-8656, Japan*

* Corresponding author.
** Corresponding author. Thermal Science and Engineering Research Group, Faculty of Mechanical and Aerospace Engineering, Institut Teknologi Bandung, 40132, Bandung, Indonesia.
E-mail addresses: firman.juangsa@itb.ac.id (F.B. Juangsa), iman.kr@universitaspertamina.ac.id, iman@ftmd.itb.ac.id (I.K. Reksowardojo).

https://doi.org/10.1016/j.csite.2024.104993

Available online 17 August 2024

G R A P H I C A L A B S T R A C T

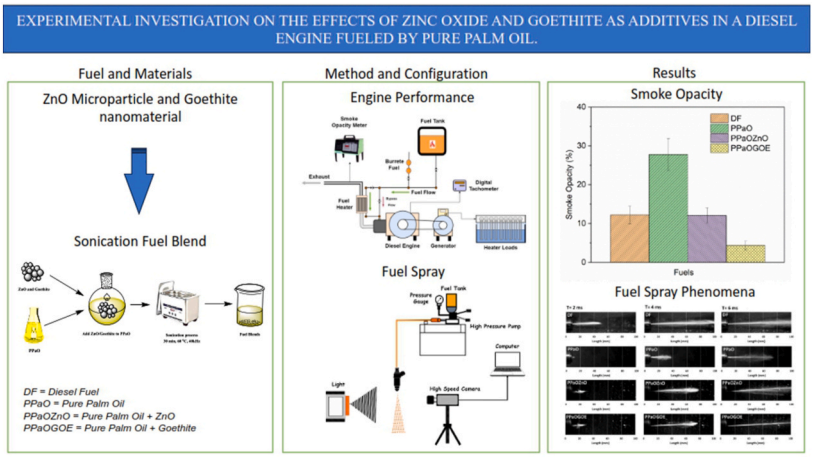

A R T I C L E I N F O

Handling Editor: Huihe Qiu

Keywords:
Pure palm oil
Zinc oxide
Goethite
Engine performance

A B S T R A C T

Recent studies have shown the potential of zinc oxide as an additive in diesel engines because of its favorable properties. Goethite, as a metal additive, exhibits good thermodynamic stability and acts as a catalyst carrier to reduce environmental pollution. Incorporating zinc oxide microparticles and goethite nanoparticles into pure palm oil (PPaO) has great potential to improve the fuel properties. Therefore, in this study, the effects of adding zinc oxide microparticles and goethite nanoparticles into PPaO on the engine performance, spray characteristics, and smoke opacity of a diesel engine were investigated. A high-speed camera was used for the spray experiments. The results showed that the use of PPaO significantly increased the smoke opacity by ~127.89 % compared with diesel fuel (DF). However, the use of PPaO with zinc oxide microparticles (PPaOZnO) and PPaO with goethite nanoparticles (PPaOGOE) significantly reduced the smoke opacity. The reduction in smoke opacity was most pronounced for the PPaOGOE fuel blend, with a value of 60 %, relative to the smoke opacity for DF. The PPaOZnO fuel blend significantly increased the specific fuel consumption by 37.1 %, with an average increase of ~24.21 %, compared with DF at an engine load of 40 %. Moreover, the use of PPaOZnO and PPaOGOE fuel blends improved spray penetration 2 times compared to PPaO, although the relative viscosity and spray angle were similar to those for PPaO. These findings suggest that zinc oxide and goethite have great potential as additives for PPaO fuel, thereby enhancing the efficiency and performance of diesel engines.

1. Introduction

In recent decades, diesel engines are preferred over gasoline engines in the mass transportation, heavy machinery, and power generation sectors due to their superior performance and robustness [1,2]. However, diesel engines emit higher levels of nitrogen oxides (NO_x), unburned hydrocarbons (UHCs), carbon monoxide (CO), soot, and particulate matter compared with gasoline engines, which necessitates efforts to reduce these emissions. One solution is to use renewable energy sources to reduce pollution and greenhouse gas emissions [3]. Biodiesels, derived from vegetable oils and animal fats through the transesterification process, are promising renewable, sustainable, biodegradable, and eco-friendly fuels, offering higher flash points, lubricity, combustion efficiency, cetane number, biodegradability, and nontoxicity compared with conventional fossil fuels [4]. It has been demonstrated that blending biodiesel with diesel fuel (DF) can reduce pollutants such as CO, carbon dioxide (CO_2), UHCs, smoke, and NO_x [5].

Pure palm oil (PPaO), derived from the oil palm tree, is a popular biofuel source, replacing conventional crude oils. Its versatile application as a feedstock for food and cosmetics and its high productivity, accounting for ~37 % of the world's vegetable oil consumption, makes it a favorable choice [6,7]. Palm oil offers the highest yield and lowest cost compared with other vegetable oils. Despite these advantages, the production of biodiesel from palm oil presents several challenges, primarily due to its complex production process [8]. Furthermore, the direct use of crude palm oil in diesel engines is not recommended because it causes undesirable effects such as higher fuel consumption, reduced engine power, and the deposition of carbon deposits in the combustion chamber [9]. Over the last two decades, numerous studies have evaluated the feasibility of using PPaO to fuel diesel engines. However, the high

viscosity of PPaO limits fuel atomization and increases fuel spray penetration, leading to lubricating oil thickening and engine deposits [10].

Considerable efforts have been made to optimize biofuel efficiency and reduce emissions, including the addition of nanoparticles into biodiesels, due to the ability of nanoparticles to achieve a more complete combustion [11]. In recent years, adding nanoparticle additives into diesel engines has gained much popularity. Sonara and Rathod [12] examined the addition of multiwalled carbon nanotubes (MWCNTs) as additives and analyzed the droplet combustion and ignition delay, including activation energy. The results showed that there was a reduction in the ignition delay and engine performance. Adding aluminum oxide (Al_2O_3) nanoparticles into DF significantly reduced NO_x, CO, UHC, and smoke emissions, leading to higher brake thermal efficiency (BTE) [13].

The effects of adding single-walled carbon nanotubes (SWCNTs), graphite oxide (GO), and cerium oxide (CeO_2) nanoparticles on the emission characteristics and combustion performance of diesel engines have been investigated in previous studies. The results revealed that nanoadditives reduced CO and UHC emissions and improved the brake specific fuel consumption (BSFC) of diesel engines. However, the addition of nanoadditives into biodiesel increased NO_x emissions compared with that for DF [14]. Adding carbon nanotubes (CNTs) into commercial diesel and palm oil biodiesel decreased ignition delay, particulate matter, and NO_x emissions in diesel engines, regardless whether the CNTs were amide-functionalized or nonfunctionalized [15]. Waste cooking oil biodiesel with TiO_2, Al_2O_3, and CNT nanoadditives enhanced the physicochemical properties of the fuel, improving thermal efficiency and decreasing CO and UHC emissions.

Nevertheless, the addition of nanoadditives increased NO_x emissions of a diesel engine fueled with waste cooking oil biodiesel [16]. The use of graphene oxide and graphite oxide in waste cooking oil biodiesel enhanced the BTE, reduced the BSFC, and reduced NO_x emissions [17]. Jatropha biodiesel added with MWCNTs, graphene nanoplatelets (GNPs), and GO showed an increase in BSFC and a reduction in the HC, NOx, and CO emissions [18].

The addition of zinc oxide (ZnO) nanoparticles into mahua biodiesel increased the BTE and decreased the BSFC, as well as reduced the smoke, UHC, NO_x, and CO emissions [19]. In addition, the incorporation of ZnO into soybean biodiesel decreased the BSFC and reduced the UHC, NO_x, CO, CO_2, and smoke emissions, as well as improved the heat release rate (HRR), mean gas temperature (MGT), and BTE [20,21]. Rajak et al. [22] investigated the effect of adding ZnO nanoadditive into DF. The results showed that the addition of ZnO nanoadditive increased the BTE and cylinder pressure, as well as reduced the BSFC and gas emissions compared with those for DF. The incorporation of ZnO nanoadditive into waste plastic oil (WPO) significantly enhanced engine performance, reduced smoke, CO, UHC, and NO_x emissions, improved the BTE by 2.47 %, and decreased the BSFC [23].

Goethite (FeOOH) is generally black in hand specimens or yellowish in massive examples. Goethite is a secondary mineral formed from the alteration of iron-rich minerals such as magnetite, siderite, pyrite, and hematite under oxidizing conditions [24]. Goethite is a stable iron oxide with favorable thermodynamic properties. Goethite can reduce the concentration of heavy metals in an aqueous solution through absorption, which is beneficial for environmental protection. In addition, goethite is used as a catalyst carrier and a precursor of nano zero-valent iron (NZVI) to reduce environmental pollution [25]. Kalishyn et al. [26] found that incorporating goethite nanoparticles as an antioxidant in gasoline fuel can significantly extend the storage period and enhance the oxidative stability of gasoline.

Nevertheless, there are limited studies on the use of PPaO as the primary fuel in indirect injection (IDI) diesel engines, incorporating zinc oxide microparticles and goethite nanoparticles as fuel additives. Most of the existing studies are focused on incorporating nanoadditives into biodiesels and DF to enhance the performance of diesel engines and reduce exhaust emissions. This study addresses the current research gap by incorporating zinc oxide microparticles and goethite nanoparticles into PPaO, which is used as the base fuel. The objective is to investigate the effects of zinc oxide microparticles and goethite nanoparticles on the performance and spray characteristics of a diesel engine in order to gain insight into how PPaO affects the combustion process.

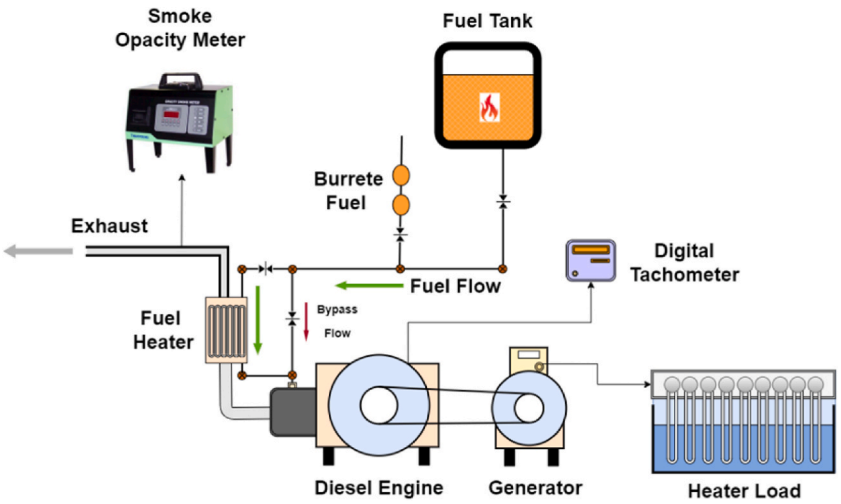

Fig. 1. Schematic diagram of the experimental setup used to determine the engine performance.

2. Materials and methods

2.1. Experimental setup used to determine the performance of the diesel engine

The diesel engine was first run to attain a stable operational state and establish an optimal working temperature environment before carrying out experiments involving PPaO and its blends. This involved operating the engine on DF for 30 min. Subsequently, the base fuel (DF) was completely purged from the fuel pump, fuel tank, and fuel lines to be substituted with the test fuels. The cooling water and lubrication oil temperatures were measured in advance to verify that the engine had achieved the appropriate warm-up condition. The engine load was increased gradually from 20 % to 100 % by modulating the current supplied to the heater load in 20 % increments. These steps were implemented, taking into account the characteristics of the diesel engine. The engine power can be determined based on the experimental results. The schematic diagram of the experimental setup is shown in Fig. 1. A smoke meter was used to measure the smoke emissions from the engine exhaust. The engine specifications are detailed in Table 1. To ensure accuracy and precision, all of the equipment and instruments were checked and calibrated before the experiments, and each operating condition was measured multiple times to minimize errors. The data were collected in triplicate after ensuring the engine had reached stable operation for at least 10 min.

2.2. Experimental setup used to determine the fuel spray characteristics

The fuel spray characteristics are of great importance to ensure proper fuel combustion and optimal diesel engine performance. In this study, an in-depth analysis was performed on the spray characteristics of the DF and PPaO and its blends using the experimental setup illustrated in Fig. 2. The specifications of the instruments are listed in Table 2. Images were captured using Phantom Miro C110 high-speed camera with a resolution of 1280 × 720 pixels and a speed of 900 fps. The experiments were conducted by varying the amount of fuel used while maintaining a constant injection pressure of 50 bar to observe the spray angle. Otsu's method was applied for the image analysis by binarizing the grayscale images, resulting in black pixels for the spray region. The spray angle was measured at a distance of 50 mm from the orifice exit.

2.3. Test fuels

In this study, the results for DF were compared with those for PPaO, PPaOZnO, and PPaOGOE. Preheating was conducted in the fuel lines at a temperature range of 60–100 °C to reduce the PPaO viscosity and avoid blockage along the fuel lines and injector, following the same procedure employed by De Almeida et al. [10]. Zinc oxide microparticles and goethite nanoparticles were used as the additive materials. Goethite was synthesized using the coprecipitation method, where $NaHCO_3$ was used as the coprecipitating agent [27]. The PPaO, zinc oxide, and goethite were mixed thoroughly by sonication, as illustrated in Fig. 3. The formulations of the test fuels are listed in Table 3, whereas the properties of the test fuels are presented in Table 4.

2.4. Fuel cost analysis

Since the PPaO was sourced locally, the cost of the oil was around $1.00–$1.20 per 8 L. The cost of the zinc oxide microparticles was $3.50 per gram, and the cost of the goethite nanoparticles was $2.00 per gram. Furthermore, the current cost of DF in Indonesia was $0.45–$1.00. The costs of the raw materials are tabulated in Table 5. The maximum fuel cost for this study was approximately $1.38, whereas the minimum cost was $1.04. Based on the fuel cost analysis, it is evident that the estimated maximum and minimum fuel costs of the PPaO and its blends were comparable to those of DF.

2.5. Uncertainty of the measurements

Uncertainty analysis is crucial to verify the credibility of the experimental results. Errors and uncertainties arise from various factors, such as instrument selection, environmental conditions, observations, and operating conditions. The uncertainties of the instruments employed in this study are summarized in Table 6. Uncertainty analysis is essential for investigative studies as it provides a detailed overview of the veracity and repeatability of the findings. The percentage experimental uncertainty was calculated using the

Table 1
Specifications of the diesel engine.

Parameters	Specification
Engine model	Dafeng S195 four-stroke diesel engine
Engine type	Indirect injection
Cooling type	Water cooling
Stroke × bore dimension	115 mm × 95 mm
Number of cylinders	Single cylinder
Compression ratio	22:1
Cylinder volume	0.815 L
Generator rated power	7500 W at 1500 rpm
Fuel capacity	5.5 L
Injection type	Mechanical pump injection
Nozzle hole	1/pintle
Engine maximum power rate	14 hp/2200 rpm
Lubricating oil	SAE 30-40
Load cell type	Heater load

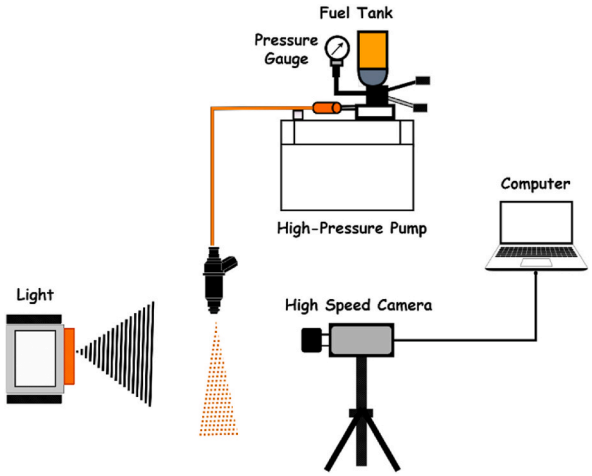

Fig. 2. Schematic diagram of the experimental setup used to determine the fuel spray characteristics.

Table 2
List of the instruments used to determine the fuel spray characteristics.

Parameters	Specification
High-speed camera	Phantom C110, 900 fps at 1280 × 1028 pixel
Nozzle type	Pintle
Maximum pressure	600 bar
Light source	GsVitec Multiled LT
Lens	Ricoh FL-CC6Z1218A-VG 12.5–75 mm 1.8 VGA
Data acquisition system	PCC Phantom

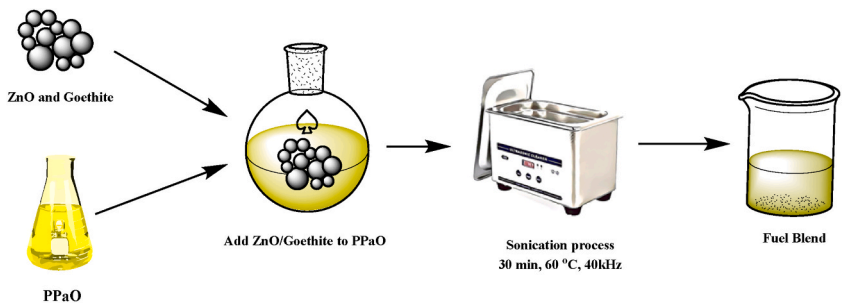

Fig. 3. Mixing of the PPaO with zinc oxide or goethite by sonication.

Table 3
Formulations of the test fuels.

Formulation	Additive Dosage	Label
Diesel Fuel	–	DF
Pure Palm Oil	–	PPaO
PPaO + ZnO	50 ppm	PPaOZnO
PPaO + Goethite	20 ppm	PPaOGOE

following equation [23,28]:

$$\frac{U_y}{y} = \sqrt{\sum_{i=1}^{n}\left(\frac{1}{y}\frac{\partial y}{\partial x_i}\right)^2} \tag{1}$$

In Equation (1), the variable y represents a specific parameter that is dependent on the value of x_i, and U_y denotes the deviation or uncertainty associated with the specific parameter y.

Table 4
Properties of the test fuels.

Test Fuel	Lower Heating Value (kcal/kg)	Density at 25 °C (kg/m^3)	Viscosity at 25 °C (cP)	Flash Point (°C)
DF	10,536	844.4	2.852	28
PPaO	9451	893.5	55.083	62
PPaOZnO	9463	889.6	52.879	49
PPaOGOE	9446	891.0	54.609	55

Table 5
Estimation of the minimum and maximum fuel costs for different test fuels.

Test Fuel	Minimum Fuel Cost ($)	Maximum Fuel Cost ($)
DF	0.45	1
PPaO	1	1.2
PPaOZnO	1.175	1.375
PPaOGOE	1.04	1.24

Table 6
Uncertainties of the instruments employed in this study.

Parameter	Accuracy	Percentage Uncertainty	Measurement Technique
Volume of test fuel	±0.1 cc	±1 %	Burette
Engine speed	±10 rpm	±0.1 %	Tachometer
Engine load	±5 W	±0.2 %	Heater load
Time	±0.1 s	±0.2 %	Stopwatch
Smoke meter	±1	±1 %	Opacity meter

Based on the uncertainties of the instruments, the percentage uncertainties of power, torque, thermal efficiency, SFC, and other parameters were determined. The uncertainties for SFC, power, torque, thermal efficiency, and smoke were ±1, ±0.2, ±0.2, ±0,2, and ±1, respectively. The total uncertainty was calculated using equation (2). The error propagation technique used in this study was referenced from previous studies [29,30].

$$\text{Total uncertainty} = \sqrt{\begin{array}{c}(\text{uncertainty of SFC})^2 + (\text{uncertainty of power})^2 + \\ (\text{uncertainty of torque})^2 + (\text{uncertainty of Thermal Efficeincy})^2 + (\text{uncertainty of Smoke Opacity})^2\end{array}} \quad (2)$$

$$\text{Total uncertainty} = \sqrt{(1)^2 + (0.2)^2 + (0.2)^2 + (0.2)^2 + (1)^2} = \pm 1.46\%$$

The total uncertainty was less than 5 %, indicating that the measured values were statistically reliable.

2.6. Characterization of the materials

The particle size distributions of the zinc oxide microparticles and goethite nanoparticles were measured using a particle size analyzer based on dynamic light scattering (Horiba Scientific SZ-100). The functional groups of the materials were characterized using a Fourier transform infrared (FTIR) spectrometer (Shimadzu IR Prestige-21). The FTIR spectrometer was operated using the KBr pellet procedure within a wavenumber range of 400 cm^{-1} and 4000 cm^{-1}. The surface morphologies of the zinc oxide microparticles and goethite nanoparticles were characterized using a scanning electron microscope (HITACHI SU3500). The samples for scanning electron microscopy (SEM) were deposited on carbon tape and then coated with gold (Au) by ion sputtering (MC1000) for 5 min. The elemental compositions of the zinc oxide microparticles and goethite nanoparticles were characterized by energy dispersive X-ray spectrometer (ZAF Smart Quant). The crystallinity of the zinc oxide microparticles and goethite nanoparticles was analyzed using an X-ray diffractometer (Bruker D8 Advance) with Cu Kα radiation (λ = 1.54060 Å).

3. Results and discussion

3.1. Zinc oxide microparticles and goethite nanoparticles

Particle size analysis (PSA) is crucial to understand the physical properties of materials. The particle size distribution is important to understand the material behavior. PSA provides the particle size distribution and is used to analyze numerous materials, including suspensions, powders, aerosols, and emulsions. Sedimentation, light propagation, and microscopy-based methods are among the PSA techniques available, each with its own advantages and disadvantages. The selection of a PSA technique is dependent on the properties of the material to be analyzed. One of these techniques is particle size analysis using light propagation, which involves analyzing the scattering of light by particles in suspension when illuminated by a laser to calculate the velocity of Brownian motion. Using the

Stokes–Einstein equation, the velocity is used to determine the particle's hydrodynamics [31]. In this study, PSA was conducted using dynamic light scattering (DLS), with a dynamic range spanning from 0.3 nm to 8 μm. The lower limit is contingent upon several factors, including the concentration of the sample, the strength of its light-scattering properties, and the presence of undesirable large particles. The density of the sample influences the upper limit since DLS is based on the principles of Brownian motion, which is in opposition to the effects of gravitational settling.

The particle size distributions of the zinc oxide microparticles and goethite nanoparticles are shown in Fig. 4. The average diameter of the zinc oxide microparticles was 154.8 nm, with a standard deviation of 46.8 nm. The average diameter of the goethite nanoparticles was 99.6 nm, with a standard deviation of 24.9 nm. Both types of materials exhibited a relatively narrow size distribution, which is a critical factor for their effective implementation.

FTIR spectroscopy is a characterization technique used to analyze chemical compounds by generating an infrared absorption spectrum. FTIR spectroscopy is used to analyze the shape of molecules and their properties. In this study, zinc oxide microparticles and goethite nanoparticles were analyzed using FTIR spectroscopy to identify the functional groups present in the materials, and the FTIR spectra are shown in Fig. 5. Based on the FTIR spectrum for zinc oxide microparticles, there were two prominent peaks within a wavenumber range of 4000 cm^{-1} to 500 cm^{-1}. These peaks represent the functional groups of zinc oxide. In addition, absorption peaks were observed at 3568, 2367, and 541 cm^{-1}. The broad peak at 3568 cm^{-1} was attributed to the stretching vibrations of the O–H bonds or hydroxyl compounds. A sharp peak at 541 cm^{-1} was ascribed to stretching vibrations of the Zn–O bonds, indicating the octahedral and tetrahedral structures of the zinc oxide microparticles. The peaks of Zn–O stretching vibrations were similar to those found by Soudagar et al. [19]. In addition, an absorption peak appeared at 2367 cm^{-1}, which can be attributed to the vibrations of CO_2 originating from the surrounding air, as shown in Table 7.

Furthermore, the FTIR spectrum of the goethite nanoparticles exhibited absorption peaks at 3138, 1600–1300, 887, 794, and 638 cm^{-1}. The broad IR band at 3138 cm^{-1} was assigned to the stretching vibrations of the H_2O compound or OH bonds. The intense band observed at 1600–1300 cm^{-1} was characteristic of NO, originating from the NO_2 precursors. This observation can be attributed to unreacted iron (II) salts, indicating that the synthesized goethite was of low purity [32]. Typical sharp bands at 887 and 794 cm^{-1} were ascribed to Fe–O–OH bending vibrations in α-FeOOH. The bands at 638 cm^{-1} were attributed to Fe–O stretching vibrations of the goethite lattice. These bands were characteristic of the goethite form [33,34].

Energy-dispersive X-ray spectroscopy (EDS) is a qualitative method used to identify the elemental compositions of the materials imaged using SEM. In this study, EDS was conducted to determine the elemental compositions of the zinc oxide microparticles and goethite nanoparticles, as shown in Fig. 6. Fig. 6(b) shows that the zinc oxide microparticles were composed of 59.1 % Zn and 40.9 % O (atomic percentage) and 85.52 % Zn and 14.48 % O (weight percentage). The EDS spectrum of goethite revealed that the yellowish-brown particles contained Fe, O, C, Na, and Mn, as presented in Fig. 6(a). The yellowish-brown nanoparticles were prepared by chemical precipitation in a rotated packed bed. The EDS spectrum revealed that the goethite nanoparticles were composed of 26.63 % Fe and 54.5 % O (atomic percentage). Other elements present in the goethite nanoparticles were C, Na, and Mn, with an atomic percentage of 16.04, 2.61, and 0.22 % respectively, which were close to the theoretical composition of goethite [35,36]. In terms of weight percentage, the yellowish-brown goethite nanoparticles were composed of 7.34 % C, 33.23 % O, 2.28 % Na, 0.45 % Mn, and 56.59 % Fe.

SEM creates images by detecting reflected or emitted electrons. SEM can be used to reveal the spatial orientations and small particle sizes of zinc oxide and goethite [37]. In this study, SEM was carried out to determine the surface morphology of the zinc oxide microparticles on a scale of 1 μm, as shown in Fig. 7(a). It can be seen that the zinc oxide microparticles were within a range of 80–200 nm, with an average particle size of 134.96 nm and standard deviation of 28.54 nm. The SEM image revealed that the zinc oxide microparticles were nearly cubical or spherical [38]. In contrast, the SEM image for the goethite nanoparticles revealed needle-like particles with a lath-like crystal habit, as shown in Fig. 7(b). The SEM image confirmed that the goethite nanoparticles had the shape of nanorods. The goethite nanoparticles had a particle size within a range of 60–120 nm, with an average particle size of 96.56

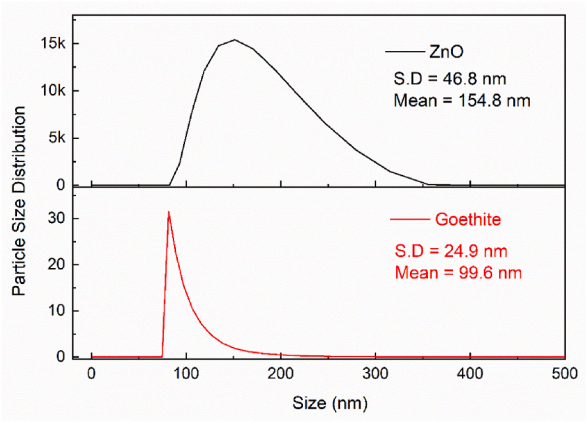

Fig. 4. Particle size distributions of the zinc oxide and goethite.

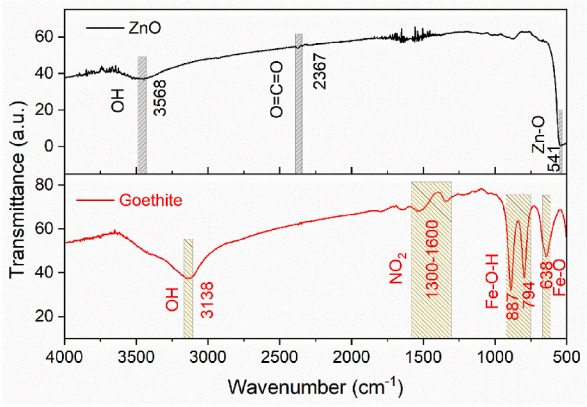

Fig. 5. FTIR spectra of the zinc oxide and goethite.

Table 7
Functional groups present in the zinc oxide and goethite identified from the FTIR spectra.

Material	Wavenumber (cm^{-1})	Functional Group
Zinc oxide	3568	OH
	2367	O=C=O
	541	Zn–O
Goethite	3138	OH
	1300–1600	NO_2
	887 and 794	Fe–O–H
	638	Fe–O

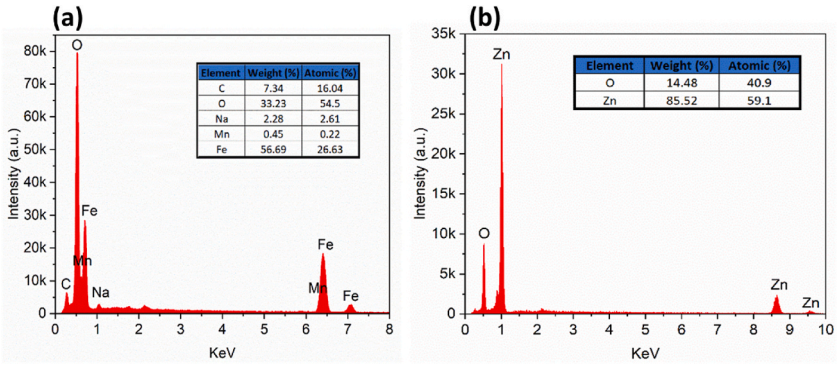

Fig. 6. Elemental compositions of (a) goethite and (b) zinc oxide obtained from EDS.

nm and standard deviation of 13.72 nm. The particle size distribution of the synthesized goethite was consistent with those of other studies [19,39,40].

X-ray diffraction (XRD) analysis is an indispensable characterization technique for obtaining intricate information on the chemical composition, crystallographic structure, and physical characteristics of materials. In this study, XRD analysis was performed on the zinc oxide microparticles and goethite nanoparticles to examine their crystal morphology and characteristic peaks. The zinc oxide and goethite additives were prepared in powder form and analyzed using an X-ray diffractometer (Bruker D8 Advance) with Cu Kα radiation. The X-ray diffractometer released radiation with λ of 1.54060 Å over a 2θ range of 10–90°, with a step size of 0.02° and a scanning rate of 0.5°/min. As shown in Fig. 8, the X-ray diffractogram of the goethite nanoparticles exhibited discernible diffraction peaks at 2θ of 21.14, 33.31, 36.6, and 53.19°, corresponding to the (110), (130), (111), and (221) crystallographic planes within the orthorhombic crystal lattice of goethite, respectively. Furthermore, the X-ray diffractogram of the zinc oxide microparticles showed distinctive diffraction peaks at 2θ of 31.74, 34.14, 36.27, 37.54, 56.57, 62.82, 66.35, 67.90, 69.08, and 76.94°, corresponding to the (100), (002), (101), (102), (110), (103), (200), (112), (201), and (202) planes of the hexagonal crystal structure of zinc oxide, respectively. The peaks observed in this study aligned with those previously reported for hexagonal zinc oxide with a wurtzite structure [41]. The X-ray diffractograms were comparable to those of previous studies [42,43]. According to the International Centre for Diffraction Data (ICDD), the results showed that the zinc oxide matched the ICDD 00-036-145 powder diffraction file, while the

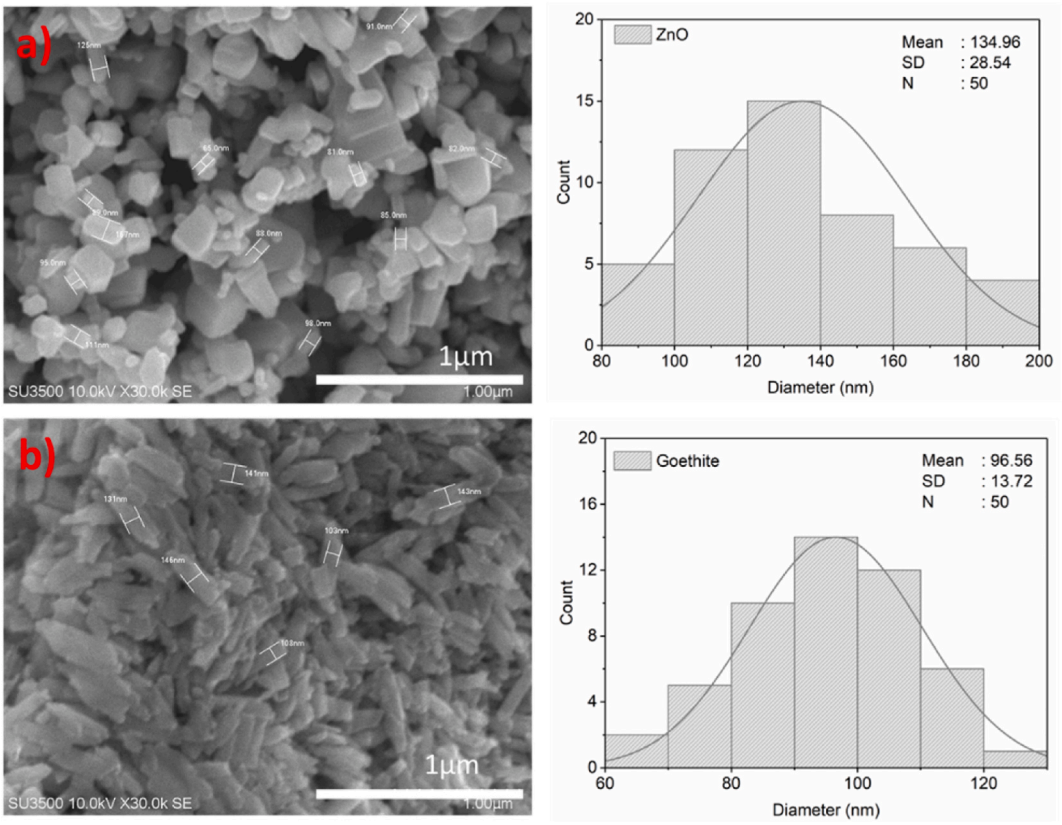

Fig. 7. SEM images and particle size distributions of the (a) zinc oxide and (b) goethite.

goethite matched the ICDD 01-081-0462 powder diffraction file.

3.2. *Effects of zinc oxide and goethite additives on the engine performance*

Engine power and torque are critical parameters that define the performance of a diesel engine. Engine power denotes the work rate executed, whereas torque represents the twisting force generated. In this study, the engine power and torque were determined based on the experimental results, as shown in Fig. 9. The results showed that the use of PPaOZnO and PPaOGOE slightly decreased the engine power and torque. The engine power decreased by an average of 4.7 and 4.9 % for PPaOZnO and PPaOGOE, respectively, relative to the engine power for DF. The engine power decreased by a maximum of 10.1 and 15.5 % for PPaOZnO and PPaOGOE, respectively, relative to engine power for DF at an engine load of 30 %. The reduced engine power and torque associated with PPaOZnO and PPaOGOE can be attributed to their lower heating values.

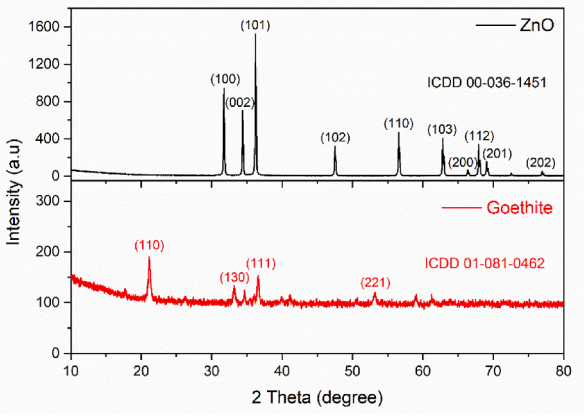

Fig. 8. X-ray diffractograms of the zinc oxide and goethite.

On the other hand, the engine power and torque increased when PPaO and PPaOGOE were used as fuels. The PPaO resulted in a maximum increase in engine power and torque of 1.3 % at an engine load of 70 %, whereas the PPaOGOE exhibited a maximum increase in engine power and torque of 1.6 % at an engine load of 20 %, compared with DF. The enhancement in engine power and torque resulting from the PPaO and PPaOGOE fuels may be attributed to the oxygen content of the fuel and the surface-to-volume ratio of the fuel additive [44]. Overall, the use of PPaOZnO and PPaOGOE slightly reduced the engine power and torque of the diesel engine compared with DF. However, it is worth noting that these fuels still yield comparable performance to DF despite the slight reduction in the engine power and torque [45].

3.3. Effects of zinc oxide and goethite additives on the fuel economy

The thermal efficiency and SFC are important parameters that determine engine performance due to their profound effect on the engine operation. Thermal efficiency is calculated as the ratio of the useful work output to the heat input. SFC indicates the fuel consumption per unit of power output.

As shown in Fig. 10(a), it can be seen that PPaOZnO resulted in the highest enhancement in SFC, with a maximum increase of 37.1 % and an average increase of ~24.21 % when operated at an engine load of 40 %, compared with DF. This is due to the fact that DF has a lower density and a higher calorific value. Therefore, PPaOZnO consumes a greater quantity of fuel in order to generate engine power that is comparable to DF [46]. Conversely, DF exhibited the lowest SFC, indicating that the diesel engine requires less fuel to produce the same power as other test fuels.

As shown in Fig. 10(b), the thermal efficiency of PPaO was comparable to that of DF. However, the PPaO increased the thermal efficiency by 10.7 % at an engine load of 10 %, whereas PPaOGOE increased the thermal efficiency by 1.23 % at an engine load of 50 %. This may be attributed to the fact that the PPaO and PPaoOGOE have a lower calorific value than DF, resulting in a reduction in the energy input to the system, while the engine power remained comparable to that of DF. These results were consistent with those of a Syarif et al. [9], who reported an increase in thermal efficiency. Overall, the use of PPaOZnO decreased the thermal efficiency, with an average decrease of 14.8 % and a maximum decrease of 22.98 % at an engine load of 40 %. The use of PPaOGOE resulted in an average decrease in thermal efficiency of 4.14 % and a maximum decrease of 11.03 % at an engine load of 30 %. A contributing factor to the observed reduction in thermal efficiency is the engine power compensation of PPaOZnO and PPaOGOE, which was slightly less than that of DF. Moreover, the lower heating value and higher density of these fuels compared with DF may also be responsible for the decrease in thermal efficiency. The results of this study were similar to those of Abed et al. [47].

In terms of the cost per kilowatt-hour (kWh), DF stood out as the most economically advantageous option across all heater load scenarios. This can be attributed to the lower SFC of DF, and therefore lower costs. However, when DF was compared with PPaO, there was a noticeable change. At engine loads above 40 %, the PPaOGOE fuel blend appeared to be a competitive substitute. This finding emphasizes the ability of the PPaOGOE to achieve an efficient balance between performance and cost-effectiveness under certain operational circumstances. This cost-effectiveness resulting from the reduced SFC of the PPaOGOE fuel blend compared with that of PPaO is shown in Fig. 11.

The interaction between the engine load and cost-effectiveness highlights a key element of engine dynamics. Because of their lower SFC, DF and PPaO are more efficient at lower loads, reducing the cost per kWh. However, when the load increases, the benefits of the PPaOGOE fuel blend become more apparent and outweigh the cost difference. This change in economic viability positions the PPaOGOE fuel blend as an economically sensible option, even if it is more expensive than PPaO and DF.

3.4. Smoke emissions

Diesel engines are known for emitting substantial volumes of particulate matter, which adversely affect human health and the environment. The opacity of exhaust smoke is a critical metric for assessing the magnitude of particulate matter emitted from diesel engines. Various factors, including extended oxidation times, insufficient oxygen levels, and elevated cylinder temperatures, jointly affect the production of exhaust emissions, with deleterious consequences on both human well-being and ecological equilibrium [48]. In this study, the use of PPaO in the IDI diesel engine significantly increased the smoke opacity by 128 %, exceeding that of DF by a significant margin, as shown in Fig. 12. This increase occurs due to the significantly higher viscosity of PPaO, which exceeds that of DF by a factor of 10, leading to the formation of larger droplets that hinder complete combustion when the fuel enters the combustion chamber. However, the introduction of PPaOZnO and PPaOGOE significantly reduced the smoke opacity, where the most pronounced reduction was observed for the PPaOGOE fuel blend, with a value of 60 %, relative to the smoke opacity for DF.

Previous investigations have demonstrated that the introduction of nanoparticle and microparticle additives into DF and biodiesels can successfully mitigate smoke opacity and CO emissions [49–51]. The incorporation of zinc oxide and goethite as additives can serve as efficacious fuel catalysts, facilitating smoother fuel droplet flow and leading to microexplosions, which result in heightened flammability and improved combustion activity. Interestingly, the use of PPaOZnO and PPaOGOE has demonstrated considerable efficacy in reducing smoke opacity and enhancing combustion efficiency of IDI diesel engines. Furthermore, the utilization of alternative energy sources infused with nanomaterials has the potential to significantly aid in the long-term mitigation of urban pollution and the depletion of conventional fuel resources.

3.5. Fuel spray characteristics

Fig. 13(a) shows that the spray characteristics of PPaO deviated from those of DF when PPaO was combined with additives due to the increase in viscosity and decrease in density. The higher viscosity of the fuel presents a challenge to fuel atomization, and the combustion process contributes to the formation of pollutants. In addition, high-viscosity fuel significantly reduces turbulence intensity, which affects the spray angle [52]. Specifically, at a pressure of 50 bar and T = 2 and 4 ms, the spray angle and penetration of

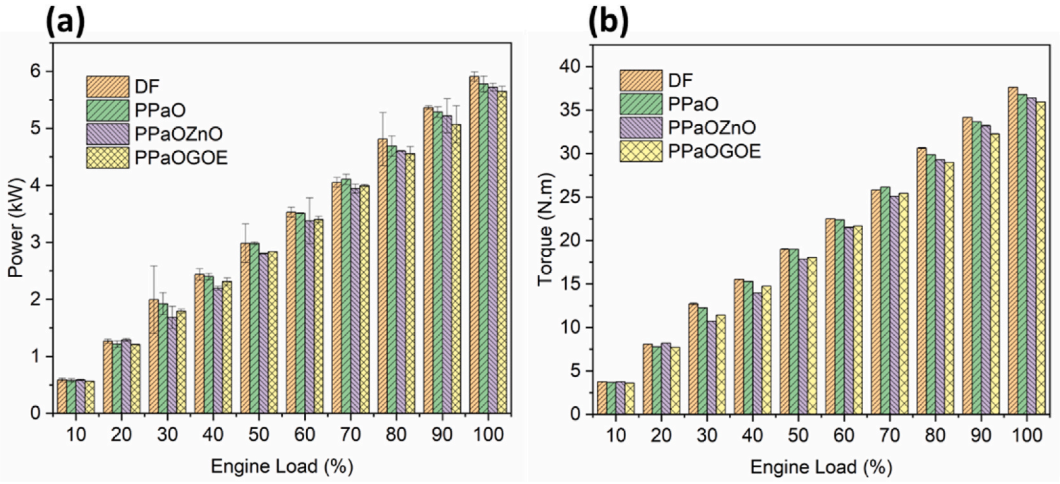

Fig. 9. (a) Engine power and (b) torque of the diesel engine fueled by different test fuels.

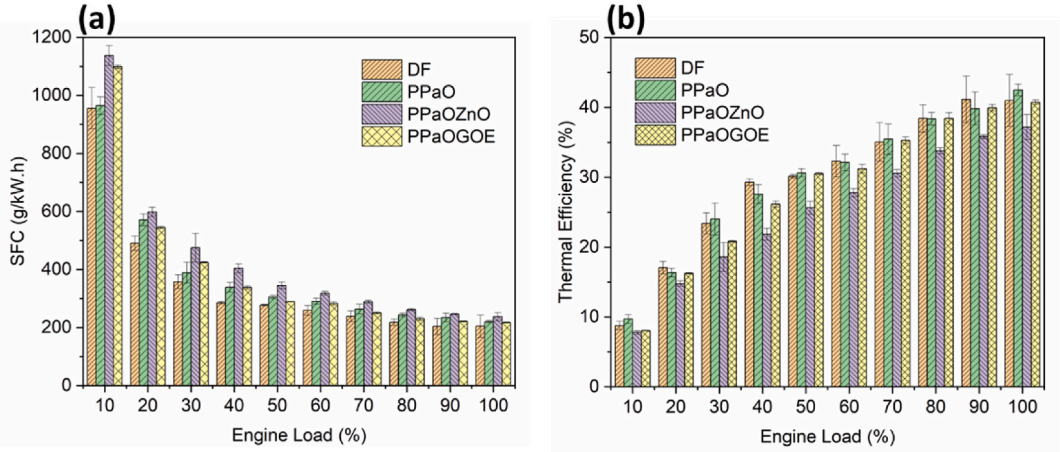

Fig. 10. (a) Specific fuel consumption and (b) thermal efficiency of the diesel engine fueled by different test fuels.

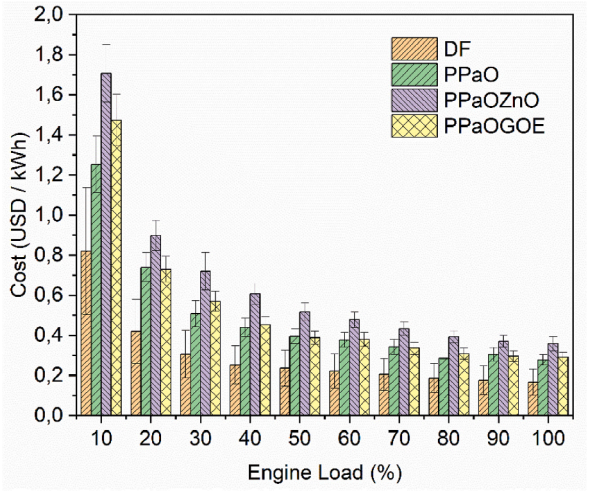

Fig. 11. Cost per kilowatt-hour of different test fuels.

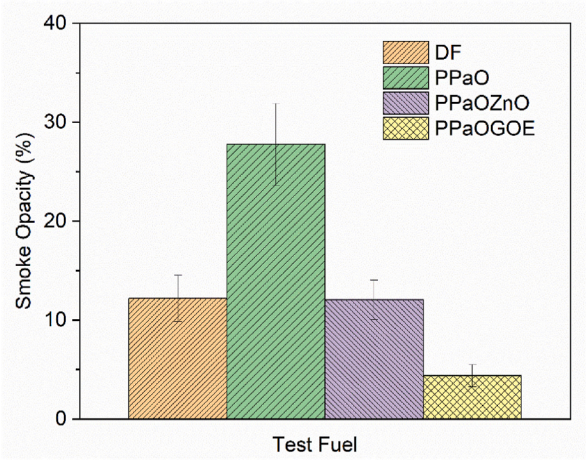

Fig. 12. Smoke opacity of different test fuels.

the PPaO spray were inferior to those of DF, suggesting deficiencies in PPaO fuel atomization. However, by incorporating additives the quality of the spray penetration was increased 2 times compared to PPaO, as evidenced from the results of the PPaOZnO and PPaOGOE fuel blends is shown in Fig. 13(a). Moreover, ss shown in Fig. 13(b), even with the addition of PPaOZnO or PPaOGOE, the spray angle characteristics were similar to those of PPaO due to their similar viscosities. The presence of additives in PPaO facilitates fuel atomization, which conforms well with the findings of Sa et al. [53], where the addition of MWCNTs into DF can increase turbulence at the nozzle outlet and decrease the spray cone angle.

4. Conclusion

The incorporation of zinc oxide and goethite as additives into PPaO fuel has the potential to enhance the fuel characteristics, specifically the lower heating value, flash point, and viscosity. The SEM images revealed a uniform distribution of zinc oxide microparticles and goethite nanoparticles within the fuel matrix, which in turn, facilitates the transfer of heat and promotes the development of a stable flame front. The results also showed a reduction in the viscosity for PPaO, PPaOZnO and PPaOGOE fuels, achieved through the application of heat prior to utilization. The introduction of PPaOZnO and PPaOGOE significantly reduced the smoke opacity, where the most pronounced reduction was achieved for the PPaOGOE fuel blend, with a value of 60 %, relative to the smoke opacity for DF. At an engine load of 10 %, the PPaO exhibited the most significant enhancement in thermal efficiency compared with DF, with a notable increase of 10.7 %. The use of PPaOGOE increased the thermal efficiency by 1.23 % at an engine load of 50 %, compared with DF. However, the use of PPaOZnO decreased the thermal efficiency, with an average decrease of 14.8 % and a maximum decrease of 22.98 % at an engine load of 40 %, compared with DF. Furthermore, the PPaOZnO fuel increased the SFC with an average increase of 24.21 % and a maximum increase of 37.1 % at an engine load of 40 %. The increase in SFC is induced by the auxiliary energy required to disintegrate the larger droplet particles in the PPaOZnO fuel blend, which reduces the overall energy efficiency of the fuel.

The quality of the fuel spray at the nozzle has a significant impact on the combustion characteristics. Therefore, it is crucial to understand the fuel spray characteristics at the nozzle in order to achieve optimal and complete combustion in diesel engines. The

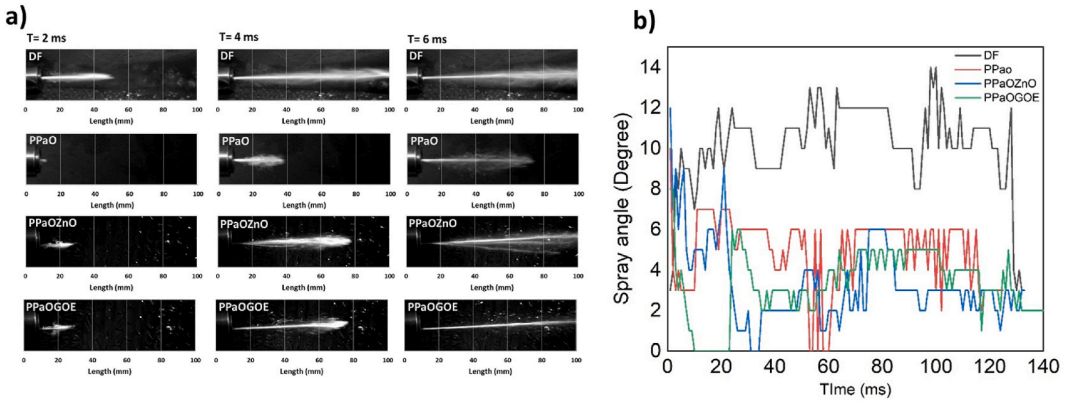

Fig. 13. (a) Fuel spray characteristics and (b) spray angle of different test fuels.

experimental results revealed that the use of PPaO reduced the spray angle and penetration compared with DF. However, the addition of zinc oxide microparticles or goethite nanoparticles into PPaO enhanced spray penetration, even though the spray angle remained unchanged, thereby facilitating fuel atomization. This highlights the potential of adding zinc oxide microparticles and goethite nanoparticles into PPaO, which enhances the combustion efficiency and performance of diesel engines.

A comprehensive understanding of the fuel spray characteristics at the nozzle is necessary to develop more efficient and environmentally friendly alternative fuels. Further studies are required to assess the advantages and constraints of this fuel strategy and to determine the optimal additive concentration that will enhance engine performance and reduce exhaust emissions for a wide variety of diesel engines, particularly in Indonesia.

CRediT authorship contribution statement

Rico Aditia Prahmana: Writing – original draft, Visualization, Methodology, Investigation, Formal analysis, Data curation, Conceptualization. **Prihadi Setyo Darmanto:** Writing – review & editing, Supervision, Funding acquisition. **Firman Bagja Juangsa:** Writing – review & editing, Supervision, Project administration, Investigation, Formal analysis. **Iman Kartolaksono Reksowardojo:** Writing – review & editing, Supervision, Conceptualization. **Tirto Prakoso:** Writing – review & editing, Supervision. **Jooned Hendrarsakti:** Validation, Supervision, Resources. **Zido Yuwazama:** Writing – review & editing, Visualization, Data curation. **Azaria Haykal Ahmad:** Writing – review & editing, Visualization, Data curation. **Teuku Meurah Indra Riayatsyah:** Writing – review & editing, Formal analysis, Data curation. **Achmad Gus Fahmi:** Writing – review & editing, Resources. **Arridina Susan Silitonga:** Writing – review & editing, Visualization, Supervision, Formal analysis. **Samsu Dlukha Nurcholik:** Writing – review & editing, Visualization.

Declaration of competing interest

The authors declare that they have no known competing financial interests or personal relationships that could have appeared to influence the work reported in this paper.

Data availability

Data will be made available on request.

Acknowledgment

This work is supported by the Asahi Glass Foundation 2024 at Institut Teknologi Bandung (ITB) for their financial support, and RAP acknowledges Institut Teknologi Sumatera (ITERA) for the doctoral program scholarship.

References

[1] P. Geng, E. Cao, Q. Tan, L. Wei, Effects of alternative fuels on the combustion characteristics and emission products from diesel engines: a review, Renew. Sustain. Energy Rev. 71 (2017) 523–534, https://doi.org/10.1016/j.rser.2016.12.080.
[2] H.A. Padmanabha, D.K. Mohanty, Impact of additive ethylene glycol diacetate on diesel engine working with jatropha-karanja dual biodiesel, Renew. Energy 202 (2023) 116–126, https://doi.org/10.1016/j.renene.2022.11.090.
[3] J.-K. Yeom, S.-H. Jung, J.-H. Yoon, An experimental study on the application of oxygenated fuel to diesel engines, Fuel 248 (2019) 262–277, https://doi.org/10.1016/j.fuel.2018.12.131.
[4] K. Abdullahi, et al., Optimization of biodiesel production from Allamanda Seed Oil using design of experiment, Fuel Communications 14 (2023) 100081, https://doi.org/10.1016/j.jfueco.2022.100081.
[5] R. Shanmuganathan, et al., Spirulina microalgae blend with biohydrogen and nanocatalyst TiO2 and Ce2O3 as step towards emission reduction: promoter or inhibitor, Fuel 334 (2023) 126791, https://doi.org/10.1016/j.fuel.2022.126791.
[6] F. Harahap, S. Leduc, S. Mesfun, D. Khatiwada, F. Kraxner, S. Silveira, Meeting the bioenergy targets from palm oil based biorefineries: an optimal configuration in Indonesia, Appl. Energy 278 (2020) 115749, https://doi.org/10.1016/j.apenergy.2020.115749.
[7] Y. Xin, L. Sun, M.C. Hansen, Oil palm reconciliation in Indonesia: balancing rising demand and environmental conservation towards 2050, J. Clean. Prod. 380 (2022) 135087, https://doi.org/10.1016/j.jclepro.2022.135087.
[8] E. Pipitone, A. Costanza, An experimental investigation on the long-term compatibility of preheated crude palm oil in a large compression ignition diesel engine, Biofuel Research Journal 5 (2018) 900–908, https://doi.org/10.18331/BRJ2018.5.4.5.
[9] A.C. Syarif, I.K. Reksowardojo, J.E. Harjono, Uji prestasi dan emisi diesel berbahan bakar minyak nabati murni untuk pembangkitan daya di daerah terpencil, Jurnal Power Plant 5 (1) (2017) 18–23, https://doi.org/10.33322/powerplant.v5i1.115.
[10] S.C. De Almeida, C.R. Belchior, M.V. Nascimento, L. dos SR Vieira, G. Fleury, Performance of a diesel generator fuelled with palm oil, Fuel 81 (16) (2002) 2097–2102, https://doi.org/10.1016/S0016-2361(02)00155-2.
[11] S. Kumar, P. Dinesha, I. Bran, Influence of nanoparticles on the performance and emission characteristics of a biodiesel fuelled engine: an experimental analysis, Energy 140 (2017) 98–105, https://doi.org/10.1016/j.energy.2017.08.079.
[12] V.D. Sonara, P.P. Rathod, Droplet combustion and ignition analysis of carbon multiwall nanotube and alumina blended jatropha biodiesel, Mater. Today: Proceedings, Tamil Nadu, India, 2021 59 (2022) (2022) 101–106, https://doi.org/10.1016/j.matpr.2021.10.210.
[13] J. Sadhik Basha, An experimental analysis of a diesel engine using alumina nanoparticles blended diesel fuel, SAE Technical Paper 2014-01-1391, 2014, https://doi.org/10.4271/2014-01-1391.
[14] J.B. Ooi, H.M. Ismail, B.T. Tan, X. Wang, Effects of graphite oxide and single-walled carbon nanotubes as diesel additives on the performance, combustion, and emission characteristics of a light-duty diesel engine, Energy 161 (2018) 70–80, https://doi.org/10.1016/j.energy.2018.07.062.
[15] J. Rentería, A. Gallego, D. Gamboa, K. Cacua, B. Herrera, Effect of amide-functionalized carbon nanotubes as commercial diesel and palm-oil biodiesel additives on the ignition delay: a study on droplet scale, Fuel 338 (2023) 127202, https://doi.org/10.1016/j.fuel.2022.127202.
[16] M. Gad, M.M.A. Aziz, H. Kayed, Impact of different nano additives on performance, combustion, emissions and exergetic analysis of a diesel engine using waste cooking oil biodiesel, Propulsion and Power Research 11 (2) (2022) 209–223, https://doi.org/10.1016/j.jppr.2022.04.004.

[17] H. Khan, et al., Effect of nano-graphene oxide and n-butanol fuel additives blended with diesel—nigella sativa biodiesel fuel emulsion on diesel engine characteristics, Symmetry 12 (6) (2020) 961, https://doi.org/10.3390/sym12060961.
[18] A.I. El-Seesy, A.M. Attia, H.M. El-Batsh, The effect of Aluminum oxide nanoparticles addition with Jojoba methyl ester-diesel fuel blend on a diesel engine performance, combustion and emission characteristics, Fuel 224 (2018) 147–166, https://doi.org/10.1016/j.fuel.2018.03.076.
[19] M.E.M. Soudagar, et al., Study of diesel engine characteristics by adding nanosized zinc oxide and diethyl ether additives in Mahua biodiesel–diesel fuel blend, Sci. Rep. 10 (1) (2020) 1–17, https://doi.org/10.1038/s41598-020-72150-z.
[20] D. Khatri, et al., Investigations for the optimal combination of zinc oxide nanoparticle-diesel fuel with optimal compression ratio for improving performance and reducing the emission features of variable compression ratio diesel engine, Clean Technol. Environ. Policy 21 (2019) 1485–1498, https://doi.org/10.1007/s10098-019-01719-8.
[21] R.S. Gavhane, et al., Effect of zinc oxide nano-additives and soybean biodiesel at varying loads and compression ratios on VCR diesel engine characteristics, Symmetry 12 (6) (2020) 1042, https://doi.org/10.3390/sym12061042.
[22] U. Rajak, Ü. Ağbulut, I. Veza, A. Dasore, S. Sarıdemir, T.N. Verma, Numerical and experimental investigation of CI engine behaviours supported by zinc oxide nanomaterial along with diesel fuel, Energy 239 (2022) 122424, https://doi.org/10.1016/j.energy.2021.122424.
[23] A. Suhel, et al., Impact of ZnO nanoparticles as additive on performance and emission characteristics of a diesel engine fueled with waste plastic oil, Heliyon 9 (4) (2023) e14782, https://doi.org/10.1016/j.heliyon.2023.e14782.
[24] S. Elias, D. Alderton, Encyclopedia of Geology, Academic Press, 2020.
[25] H. Liu, T. Chen, R.L. Frost, An overview of the role of goethite surfaces in the environment, Chemosphere 103 (2014) 1–11, https://doi.org/10.1016/j.chemosphere.2013.11.065.
[26] Y. Kalishyn, E. Polunkin, P. Strizhak, Enhancement in the oxidative stability of commercial gasoline fuel by the goethite nanoparticles. https://doi.org/10.26434/chemrxiv.7048781.v1, 2018.
[27] S. Krehula, S. Popović, S. Musić, Synthesis of acicular α-FeOOH particles at a very high pH, Mater. Lett. 54 (2–3) (2002) 108–113, https://doi.org/10.1016/S0167-577X(01)00546-8.
[28] M.E.M. Soudagar, N.N. Nik-Ghazali, M.A. Kalam, I.A. Badruddin, N.R. Banapurmath, M.A.B. Ali, N. Akram, An investigation on the influence of aluminium oxide nano-additive and honge oil methyl ester on engine performance, combustion and emission characteristics, Renew. Energy 146 (2020) 2291–2307, https://doi.org/10.1016/j.renene.2019.08.025.
[29] R. Vallinayagam, S. Vedharaj, W. Yang, P. Lee, K. Chua, S. Chou, Combustion performance and emission characteristics study of pine oil in a diesel engine, Energy 57 (2013) 344–351, https://doi.org/10.1016/j.energy.2013.05.061.
[30] R.A. Prahmana, et al., The influence of acetylene black microparticles as a fuel additive in pure palm oil and its performance characteristic on diesel engine, Results in Engineering (2024) 102390, https://doi.org/10.1016/j.rineng.2024.102390.
[31] R. Hussain, et al., An ultra-compact particle size analyser using a CMOS image sensor and machine learning, Light Sci. Appl. 9 (1) (2020) 21–31, https://doi.org/10.1038/s41377-020-0255-6.
[32] D. Kharisma, Z. Abidin, C. Kusmana, Adsorption of methylene blue onto a low-cost and environmental friendly goethite, IOP Conf. Ser. Earth Environ. Sci. 399 (1) (2019) 012013, https://doi.org/10.1088/1755-1315/399/1/012013. IOP Publishing.
[33] H. Cui, W. Ren, P. Lin, Y. Liu, Structure control synthesis of iron oxide polymorph nanoparticles through an epoxide precipitation route, J. Exp. Nanosci. 8 (7–8) (2013) 869–875, https://doi.org/10.1080/17458080.2011.616541.
[34] F. Salimi, H. Rahimi, C. Karami, Removal of methylene blue from water solution by modified nanogoethite by Cu, Desalination Water Treat. 137 (2019) 334–344, https://doi.org/10.5004/dwt.2019.23635.
[35] C.-C. Lin, J.-H. Lin, K.-Y. Wu, Preparation of nanostructured goethite by chemical precipitation in a rotating packed bed, Ceram. Int. 49 (2) (2023) 1874–1879, https://doi.org/10.1016/j.ceramint.2022.09.151.
[36] G.-t. Zhou, et al., Enhanced conversion mechanism of Al-goethite in gibbsitic bauxite under reductive Bayer digestion process, Trans. Nonferrous Metals Soc. China 32 (9) (2022) 3077–3087, https://doi.org/10.1016/S1003-6326(22)66004-7.
[37] C. Hansel, S. Benner, J. Neiss, A. Dohnalkova, R. Kukkadapu, S. Fendorf, Secondary mineralization pathways induced by dissimilatory iron reduction of ferrihydrite under advective flow, Geochem. Cosmochim. Acta 67 (2003) 2977–2992, https://doi.org/10.1016/S0016-7037(03)00276-X.
[38] R.H. Vali, et al., Optimization of variable compression ratio diesel engine fueled with Zinc oxide nanoparticles and biodiesel emulsion using response surface methodology, Fuel 323 (2022) 124290, https://doi.org/10.1016/j.fuel.2022.124290.
[39] Y.N. Kanafin, P. Abdirova, E. Arkhangelsky, D.D. Dionysiou, S.G. Poulopoulos, UVA and goethite activated persulfate oxidation of landfill leachate, Chemical Engineering Journal Advances (2023) 100452. https://colab.ws/articles/10.1016/j.ceja.2023.100452.
[40] V. Zin, et al., Effect of external magnetic field on tribological properties of goethite (a-FeOOH) based nanofluids, Tribol. Int. 127 (2018) 341–350, https://doi.org/10.1016/j.triboint.2018.06.023.
[41] R.N. Moussawi, D. Patra, Modification of nanostructured ZnO surfaces with curcumin: fluorescence-based sensing for arsenic and improving arsenic removal by ZnO, RSC Adv. 6 (21) (2016) 17256–17268, https://doi.org/10.1039/C5RA20221C.
[42] V.B. Patil, M.M. Shanbhag, R.R. Sawkar, S.M. Tuwar, N.P. Shetti, ZnO interrelated graphene matrix-based sensors for quercetin, Mater. Chem. Phys. 296 (2023) 127238, https://doi.org/10.1016/j.matchemphys.2022.127238.
[43] H. Liu, X. Lu, E.D. Flynn, J.G. Catalano, Fate of arsenic during the interactions between Mn-substituted goethite and dissolved Fe (II), Geochem. Cosmochim. Acta 356 (2023) 1–13, https://doi.org/10.1016/j.gca.2023.06.028.
[44] A. Heidari-Maleni, T.M. Gundoshmian, B. Karimi, A. Jahanbakhshi, B. Ghobadian, A novel fuel based on biocompatible nanoparticles and ethanol-biodiesel blends to improve diesel engines performance and reduce exhaust emissions, Fuel 276 (2020) 118079, https://doi.org/10.1016/j.fuel.2020.11807.
[45] S. Hoseini, G. Najafi, B. Ghobadian, M. Ebadi, R. Mamat, T. Yusaf, Biodiesels from three feedstock: the effect of graphene oxide (GO) nanoparticles diesel engine parameters fuelled with biodiesel, Renew. Energy 145 (2020) 190–201, https://doi.org/10.1016/j.renene.2019.06.020.
[46] S. Radhakrishnan, D.B. Munuswamy, Y. Devarajan, A. Mahalingam, Effect of nanoparticle on emission and performance characteristics of a diesel engine fueled with cashew nut shell biodiesel, Energy Sources, Part A Recovery, Util. Environ. Eff. 40 (20) (2018) 2485–2493, https://doi.org/10.1080/15567036.2018.1502848.
[47] K. Abed, A.K. El Morsi, M.M. Sayed, A. El Shaib, M. Gad, Effect of waste cooking-oil biodiesel on performance and exhaust emissions of a diesel engine, Egyptian journal of petroleum 27 (4) (2018) 985–989, https://doi.org/10.1016/j.ejpe.2018.02.008.
[48] J. Lv, S. Wang, B. Meng, The effects of nano-additives added to diesel-biodiesel fuel blends on combustion and emission characteristics of diesel engine: a review, Energies 15 (3) (2022) 1032, https://doi.org/10.3390/en15031032.
[49] T. Shaafi, R. Velraj, Influence of alumina nanoparticles, ethanol and isopropanol blend as additive with diesel–soybean biodiesel blend fuel: combustion, engine performance and emissions, Renew. Energy 80 (2015) 655–663, https://doi.org/10.1016/j.renene.2015.02.042.
[50] A. Prabu, Nanoparticles as additive in biodiesel on the working characteristics of a DI diesel engine, Ain Shams Eng. J. 9 (4) (2018) 2343–2349, https://doi.org/10.1016/j.asej.2017.04.004.
[51] R. Gavhane, et al., Influence of silica nano-additives on performance and emission characteristics of Soybean biodiesel fuelled diesel engine, Energies 14 (5) (2021) 1489, https://doi.org/10.3390/en14051489.
[52] D. Shao, et al., Prediction of the fuel spray characteristics in the combustion chamber with methane and TiO2 nanoparticles via numerical modelling, Fuel 326 (2022) 124820, https://doi.org/10.1016/j.fuel.2022.124820.
[53] B. Sa, V. Markov, Y. Liu, V. Kamaltdinov, W. Qiao, Numerical investigation of the effect of multi-walled carbon nanotube additive on nozzle flow and spray behaviors of diesel fuel, Fuel 290 (2021) 119802, https://doi.org/10.1016/j.fuel.2020.119802.